Fabrication and characterization of thin self-rolling film for anti-inflammatory drug delivery

Sidzigui Ouedraogo, Mathilde Grosjean, Isabelle Brigaud, Katia Carneiro, Valeriy Luchnikov, Noelle Mathieu, Xavier Garric, Benjamin Nottelet, Karine Anselme, Laurent Pieuchot, et al.

Colloids and Surfaces B: Biointerfaces 241 (2024) 114039

Contents lists available at ScienceDirect

Colloids and Surfaces B: Biointerfaces

journal homepage: www.elsevier.com/locate/colsurfb

Fabrication and characterization of thin self-rolling film for anti-inflammatory drug delivery

Sidzigui Ouedraogo [a], Mathilde Grosjean [b], Isabelle Brigaud [a], Katia Carneiro [e], Valeriy Luchnikov [a], Noëlle Mathieu [c], Xavier Garric [b,d], Benjamin Nottelet [b,d], Karine Anselme [a], Laurent Pieuchot [a], Arnaud Ponche [a,1,*]

[a] Institut de Science des Matériaux de Mulhouse, Université de Haute-Alsace, CNRS/UHA UMR 7361, Mulhouse, France
[b] Polymer for Health and Biomaterials, IBMM, Université de Montpellier, CNRS, ENSCM, Montpellier, France
[c] Institute for Radioprotection and Nuclear Safety, (IRSN), PSE-SANTE/SERAMED/LRMed, Fontenay-aux-Roses F-92262, France
[d] Department of Pharmacy, Nîmes University Hospital, Nimes, France
[e] Graduate School in Pathological Anatomy and Morphological Sciences, Federal University of Rio de Janeiro, Brazil

ARTICLE INFO

Keywords:
Drug delivery
Self-rolling bilayer
Thin films
Anti-inflammatory
8 arm star copolymer

ABSTRACT

Thin films have been identified as an alternative approach for targeting sensitive site as drug delivery tool. In this work, the preparation of self-rolling thin films to form tubes for wound healing and easy placement (e.g. in the colon via colonoscopy) have been studied. We explored the use of thin films as a protective dressing combined to local release of an anti-inflammatory in order to improve drug efficacy and limit the side effects of the oral route. Non-cytotoxic poly(ethylene) glycol and poly(lactic acid) photo-crosslinkable star copolymers were used for rapid UV crosslinking of bilayered films loaded with prednisolone. The films, crosslinked under UV lamp without the need of photoinitiator, are optimized and compared in terms of water uptake, swelling ratio, final tube diameter and morphology, anti-inflammatory drug loading and release. Our studies showed the spontaneous rolling of bilayer constructs directly after immersion in water. Tubular geometry allows application of the patch through minimally invasive procedures such as colonoscopy. Moreover, the rolled-up bilayers highlighted efficient release of encapsulated drug following Fickian diffusion mechanism. We also confirmed the anti-inflammatory activity of the released anti-inflammatory drug that inhibits the pro-inflammatory cytokine IL-1β in RAW 264.7 macrophages stimulated by Escherichia coli (*E. coli*).

1. Introduction

Radiotherapy is an effective technique for the management of many cancers and around 30 % of patients are treated for pelvic tumor. Despite much progress in radiotherapy protocols, treatment with external radiotherapy leads to exposure of healthy tissues surrounding the tumor to ionizing irradiation. Due to the high proliferation capacity of epithelial cells, the colon is affected by treatment of pelvic area cancers [1]. Radiation-related toxicity induces crypt cell apoptosis, leading to mucosal lesions with a loss of epithelial barrier function associated with chronic inflammation that prevents the tissue from renewing itself. Today, the contemporary vision of radiation intestinal or colorectal pathogenesis is integrated and involves multiple cell compartments that interact in a complex sequence of events following the radiation insult. Thus, the immune system, enteric nervous system, macrovascular and microvascular systems, mesenchymal and epithelial cells, and even gut microbiome can contribute to the initiation and progression of radiation-induced intestinal injury [1–3]. Gastrointestinal radiation toxicity was recently recognized as a new pathology called “pelvic radiation disease” by Andreyev et al. in 2010 [4] as the result of multiple and sequential organ dysfunctions making the development of therapeutic strategies complex. Currently there is no curative treatment for this disease. Only symptoms are treated, for example, through long systemic anti-inflammatory drugs treatment to aid tissue renewal by reducing the inflammation and to accelerate the return to homeostasis [5,6]. However, such long lasting oral administration of anti-inflammatory drugs can cause severe side effects in the gastrointestinal tract enhancing gastritis, peptic ulceration, and gastrointestinal

* Corresponding author.
E-mail address: arnaud.ponche@uha.fr (A. Ponche).
[1] https://orcid.org/0000–0002-8993–2896.

https://doi.org/10.1016/j.colsurfb.2024.114039
Received 23 February 2024; Received in revised form 10 June 2024; Accepted 12 June 2024
Available online 13 June 2024

hemorrhage, as well as in the liver, and kidneys [7]. Therefore, local delivery of low doses of anti-inflammatory drugs could provide a sustained response and minimize systemic side effects. We investigated the design of a thin film that can act as a dressing to protect the inflamed area and deliver anti-inflammatory drugs locally. In order to facilitate the placement into the colon and simplify the surgical procedure, we targeted the design of enrolling thin films to form a tube that could be easily inserted via colonoscopy.

Various type of polymer platforms encountering shape changes in response of a stimuli such as temperature [8] or pH [9] have been developed for the administration of pharmaceutical drugs but remain of limited applicability due to the sensitivity of cells or active molecules to these stimuli. Models based on fast water responsive rolling appear more attractive. Such models rely on the fabrication of bilayered structures with different swelling and mechanical properties generating in aqueous solution a differential deformation in the layers and consequently their self-rolling [10,11]. PLA is a synthetic biodegradable polymer. It hydrolyzes into nontoxic hydroxyl-carboxylic acid through ester bond cleavage metabolized into water and carbon dioxide through a citric acid cycle. Due to its suitable biodegradability, good security, low immunity, and good mechanical strength, PLA has been approved by the US Food and Drug Administration for application in tissue engineering, medical materials, drug carriers. However, PLA applications are limited due to its weak hydrophilicity, long degradation time and low loading of polar drugs [12]. On the other hand, polyethylene glycol (PEG), a biocompatible hydrophilic non-degradable polymer approved by the US Food and Drug Administration presents many advantages. Through copolymerization PLA can be associated to PEG in order to improve its hydrophilicity, degradation rate, crystallization and mechanical properties showing great potential for development in drug delivery [13]. We previously reported the use of star-shaped PEG-PLA copolymers to prepare non-cytotoxic hydrophilic and hydrophobic layers entering in the fabrication of bilayered films able to enroll upon hydration [14] (fig. S1). The advantage of the tubular structure is primarily related to the ease of application and manipulation of the patch with surgical tools. tubes can be delivered through minimally invasive procedures such as colonoscopy clamps. The small size and geometry of the rolled patch is then effective in bringing the patch to the good site and unrolling the patch over the injured area. The aim of this work is to take advantage of this platform to make it suitable for self-rolling tubes for anti-inflammatory drug delivery.

We first chose to work with prednisolone, a corticosteroid drug widely used for immune suppression already administrated in the treatments for gastrointestinal symptoms associated with radiotherapy [6]. This pharmaceutical molecule helps to promote return to homeostasis by down-regulation of key pro-inflammatory genes expression [tumor necrosis factor-a (TNF-α), interleukin-1β (IL-1β), and IL-6] and upregulation of anti-inflammatory genes [IL-10, Cluster of Differentiation 206] via binding to glucocorticoid receptors expressed ubiquitously in almost every human cell, including all immune cells [15,16].

We then discuss the design parameters of the bilayered films (size, thickness) and the loading parameters of the prednisolone to yield fast rolling anti-inflammatory loaded tubes. The optimized dressings achieve a fast self-rolling in less than 30 s, and an efficient drug release following Fickian diffusion mechanism with release amounts that can be adjusted by varying the quantity of drug dissolved in loading buffers in which films are immersed. We finally show that the released drug is pharmacologically active by down-regulating pro-inflammatory gene expression in macrophages in response to a simulated bacterial infection. Our findings show that the developed platform can be addressed for local anti-inflammatory drug delivery in the colon to minimize side effects of systemic administrations.

2. Material and methods

2.1. Materials

UV crosslinkable star-shaped copolymers composed of a poly (ethylene glycol) 8 arms central block (PEG) associated with side blocks of poly (lactic acid) (PLA) end-functionalized with methacrylic groups were synthesized using the protocol described in our previous study [14]. $PEG_{8arm}20k\text{-}(PLA_{13})_8$ copolymer was prepared as the hydrophilic copolymer, while $PEG_{8arm}10k\text{-}(PLA_{69})_8$ copolymer was aimed as the hydrophobic one. Dichloromethane, Phosphate Buffered Saline (PBS), acetonitrile (ACN, CHROMASOLV Plus, HPLC grade), ethanol (EtOH) 96 %, the anti-inflammatory molecule prednisolone (PDS; M=360.44 g. mol^{-1}), the Dulbecco's modified Eagle's medium (DMEM) high glucose, the accutase and the Penicillin/Streptomycin were obtained from Sigma Aldrich (Saint-Quentin-Fallavier, France). The fetal bovine serum (FBS) was purchased from Thermo Fisher Scientific (Illkirch-Graffenstaden, France).

2.2. Methods

2.2.1. Fabrication of PEG-PLA-based films

Monolayers $PEG_{8arm}10k\text{-}(PL_{69})_8$ (H^-L) and $PEG_{8arm}20k\text{-}(PLA_{13})_8$ (H^+L) films were prepared by simple casting and UV-photo crosslinking of dry polymer in molds according to our previous study [14]. The precursor solution was prepared by mixing the polymers in dichloromethane. Afterwards, it was poured in aluminum cup molds (43 mm diameter) and the solvent was let to evaporate slowly. The resulting polymer were irradiated under UV light at a wavelength of 365 nm and a power of 74 mW/cm^2 for 10 min (Fig. 1).

Depending on the hydrophilicity of the copolymers, the crosslinked layers show a linear degradation in about 50 days for the hydrophilic layer (H^+L) against 150 days for the hydrophobic one (H^-L) under physiological mimicking conditions (phosphate saline buffer, pH 7.4, 37°C) (Figure S2a). Of notice the copolymers were not cytotoxic according to ISO-10993 standard with L929 murine fibroblasts viability above the threshold of 70 % (Figure S2b).

The bilayer films were prepared using a 2-step simple casting method. The H^-L polymer solution was poured in the aluminum cup mold and the dichloromethane was let to evaporate slowly. Then, the H^+L precursor solution was poured onto the dry H^-L layer and the dichloromethane was let to evaporate slowly. The resulting polymer bilayer were irradiated under UV light with a wavelength of 365 nm and a power of 74 mW/cm^2 for 10 min. The bilayer substrates obtained were cut into rectangular shapes of 1.5 cm. x 1 cm. Mechanical stability, self-rolling kinetics and degradability of the bilayers (fig. S5) are described in ref. [14],

The samples were dried for 24 h at 37°C then weighed (W_{d1}) and immersed in dichloromethane (5 mL) in order to remove non crosslinked soluble fractions. The films were then removed from dichloromethane, dried at 37°C for 24 h and weighed (W_{d2}). The gel fraction was determined using Eq. (1) as shown below:

$$\text{Gel fraction}(\%) = \frac{W_{d2}}{W_{d1}} \times 100. \quad (1)$$

2.2.2. Equilibrium Water Content

Water uptake kinetics were investigated by immersing the dry films of known mass (W_{d2}) in PBS 1X (pH = 7.4) at 37°C. The films were withdrawn from buffer solutions at different times and the excess solvent droplets on the surface were removed carefully, then the samples were weighted (W_t), and re-immersed in the buffer to achieve equilibrium swelling. The percentage of water content of each sample based on mass was calculated using following Eq. (2):

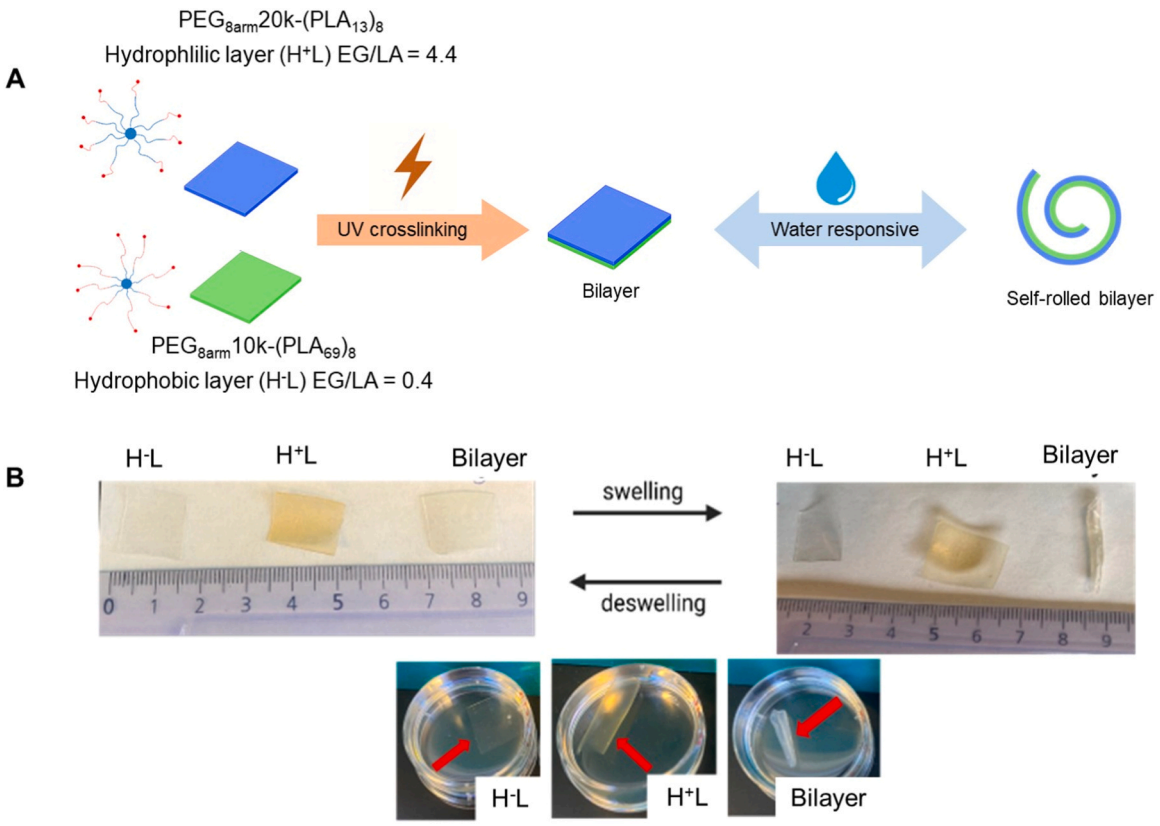

Fig. 1. A- Schematic representation of monolayer and bilayer preparation. B- Photographs of dry films obtained after crosslinking (left picture), and of films after immersion in water, with self-rolling of bilayer in contrast to monolayer H⁻L and H^{+}L (right and bottom pictures).

$$EWC_{(t)}(\%) = \frac{W_t - W_{d2}}{W_{d2}} \times 100. \quad (2)$$

The water content at the equilibrium state is calculated using the film weight at its equilibrium swollen state using Eq. (3):

$$EWC_{(s)}(\%) = \frac{W_s - W_{d2}}{W_{d2}} \times 100 \quad (3)$$

where W_S is the film mass after swelling.

Eq. 3 were also used to calculate the ethanol solvent content at equilibrium swelled state, replacing water with ethanol.

2.2.3. Measurement of Thickness

Film thicknesses were measured using a digital micrometer (MITUTOYO 293–501) at 3 positions on each film that were randomly selected and the average of 3 values were reported as the thickness (T) of the film.

2.2.4. Drug loading and release

Dry films were immersed in Prednisolone solutions and the drug was allowed to diffuse into the films for 24 h at 37°C. Different loading buffers were used, such as water and ethanol. The drug release from the loaded sample films were studied in 10 mL of PBS 1X buffer with pH 7.4 at 37°C. The release concentrations were determined using Reverse Phase High Performance Liquid Chromatography equipped with Column Poroshell 120 EC-C18 (3×50 mm) 2.7 μm diameter from Agilent Technologies, using a mobile phase consisting of water and acetonitrile in a volumetric ratio of 70:30 at a flow rate of 0.2 mL/min. Signals of prednisolone were recorded using DAD UV detector at 247 nm in a 1100 Agilent chromatographic system.

The quantification and detection limits were calculated on the basis of the standard deviation of the response and the slope obtained from regression line as described in the relevant ICH guidelines[17].

Drug release data were analyzed according to the Korsmeyer-Peppas Curve Fitting Analysis equation as shown below[18]:

$$\frac{M_t}{M_\infty} = Kt^n \quad (4)$$

where M_t is the amount of drug released at time t, M_∞ is the amount of drug released at infinite time, K is the constant related to the structural and geometric characteristics of the drug delivery system, and n is the release exponent indicative of the release mechanism. The optimum values for the parameters present in the equation were determined using the Origin Software (Origin(Pro), Version *2022,* OriginLab Corporation, Northampton, MA, USA).

2.2.5. Measurement of anti-inflammatory activity

Anti-inflammatory properties were evaluated *in vitro* using RAW 264.7 mouse macrophages by stimulating inflammation after direct contact with *E. coli* BL 21 strain. The assay consisted of measuring pro-inflammatory cytokine IL-1β gene expression regulation in cells co-cultured with bacteria strain and treated with medium containing prednisolone for 18 hours. Before macrophage exposure to the bacterial strain, the prepared bilayers were immersed in prednisolone solution for loading, as described above in order to assess the desired amount after 24 hours of release. Then the loaded bilayers were re-immersed in complete culture medium. After 24 hours, medium containing the released prednisolone was collected and filtered for cell treatment.

2.2.5.1. Macrophages Culture. Murine macrophage-like RAW 264.7 cells (CLS Cell Lines Service, Eppelheim, Germany) were cultivated in Dulbecco's modified Eagle's medium (DMEM) high glucose supplemented with 10 % fetal bovine serum and 1 % Penicillin/Streptomycin in a humidified incubator at 37°C and 5 % CO_2. Cells were seeded at 10^6 RAW 264.7 macrophages on 25 cm^2 flasks and once they reached 80–90 %, they were detached using accutase following the procedure

provided by the supplier. The cell concentration was then adjusted for further use.

2.2.5.2. Bacterial culture. *E. coli* BL 21 bacteria strain was obtained from Invitrogen (France). Bacteria were cultured in Lysogeny broth (LB) medium + 0.1 % of ampicillin at 37 °C for 18 h until the start of stationary phase. Afterward, bacterial cells were centrifuged and washed twice in PBS 1X and viable counts adjusted to a density of 1.5×10^8 CFUs/mL.

2.2.5.3. Macrophage Exposure to Bacteria. Before macrophages seeding, 6-wells culture plates were treated with 0.001 % (v/v) of poly(L-lysine) coating for at least for 40 minutes for bacteria immobilization. Then bacteria were re-suspended and seeded (37.5×10^6 CFUs/well) on poly (L-lysine)-treated wells and allowed to attach for 40 min. The wells were then washed with PBS 1X and the RAW 264.7 cells were seeded at 5×10^5 cells/well on the pre-treated plates with poly(L-lysine) containing bacteria and were incubated for 18 hours in a media containing prednisolone. A multiplicity of infection (MOI) of 75:1 (bacteria: cells) was defined after optimization following [19]. Then, the media was removed and the wells were washed with PBS 1X, and finally, the RNA was extracted for qPCR analysis.

2.2.5.4. Reverse transcription and quantitative real time polymerase chain reaction (RT-qPCR). Total RNA was extracted using Qiagen RNeasy micro kit (deoxyribonuclease treatment included) and cDNA was synthesized from 1 μg RNA with the iScript cDNA Synthesis kit (BioRad). Quantitative PCR was performed and the expression of IL-1β mRNA was quantified using the SYBR Select Master Mix (Life Technologies) and measured with the CFX384 system (BioRad).

The real time quantitative PCR data was analyzed following the $2^{-\Delta\Delta Ct}$ method as described by Livak and Schmittgen [20] using Rplp0 as an housekeeping gene. Thus, the relative amount of the target transcript is described as fold increase (RQ, relative quantification) relative to the reference sample and Rplp0 using biological triplicates and technical duplicates for each experimental group. The primer sequences were: RPLP 5'-0: ACCTCCTTCTTCCAGGCTTT- 3' and 5'-TCAGCATGTTCAGCAGTGTG-3', Il-1β: 5'- TG CCACCTTTTG ACA GTGATG-3' and 5'-AAGGTCCACGGGAAAGACAC-3'.

Experimental groups:

- RAW 264.7 cells + culture medium
- RAW 264.7 cells + culture medium + Bacteria strain
- RAW 264.7 cells + culture medium + Bacteria strain + prednisolone in solution at 30 μM
- RAW 264.7 cells + culture medium + Bacteria strain + prednisolone released from bilayer at 25 μM
- RAW 264.7 cells + culture medium + Bacteria strain + prednisolone released from bilayer at 12 μM

2.2.6. Statistical analysis

Statistical analyses were performed with Graph Pad Prism 9.0 software and the tests applied to each dataset were detailed in the corresponding figure legends. Comparisons between two samples were performed with two-tailed Student's *t*-test. Comparisons between multiple samples were performed by one-way analysis of variance (ANOVA) after a Shapiro-Wilk test for normality. The subgroups were compared by a *post hoc Tukey* test. Statistical significance was set at a probability of $p < 0.05$.

3. Results and discussion

3.1. Preparation of UV-cross-linked PEG-PLA-based films and self-rolling

Methacrylated star copolymers were used to prepare cross-linked networks. There are several factors that need to be considered for the effective incorporation and drug release by the thin films. The first one is the stability of the thin films carrying drugs [21]. The most typical approach for preparing thin films is simple casting [22]. For monolayers preparation, after solubilization, methacrylated PEG-PLA based copolymers were poured into aluminum molds. Before exposure to UV light, the solvent was allowed to evaporate in the dark. This method associated with the multi-functionality of the star copolymers (8 methacrylate per star) permits the rapid fabrication of non-cytotoxic films without adding any photocrosslinker [14] (Fig. 1). Indeed, cell viability assays performed on mouse fibroblast L929 cells following ISO 10993–12 recommendations highlighted the non-cytotoxicity of PEG-PLA copolymers films. In line with our previous results, calculated gel fraction exceeded 85 % for each fabricated batch which confirm the high crosslinking efficiency of star-shaped copolymers to form stable 3D matrices (Table S1). $PEG_{8arm}10k\text{-}(PLA_{69})_8$ (H^-L) showed a slightly lower gel fraction, presumably due to its higher molecular weight compared to $PEG_{8arm}20k\text{-}(PLA_{13})_8$ (H^+L) (50000 g/mol *vs* 27500 g/mol) [14].

Swelling of films was explored in PBS 1X (pH = 7.4) at 37°C. The water uptake increased and begun to stabilize after the first hour. After 5 hours, the water content begun to drop to an equilibrium value as shown in Fig. 2A. Analysis of equilibrium water content (%) showed the difference between the H^-L and H^+L polymer. In more details, the H^-L layer composed of $PEG_{8arm}10k\text{-}(PLA_{69})_8$ showed a lower water uptake of 17 ± 3 %, compared to H^+L composed of $PEG_{8arm}20k\text{-}(PLA_{13})_8$ (EWC of 151 ± 3 %). The formed bilayer undergoes a median equilibrium water content with 84 ± 16 % (Fig. 2B). As observed in the photograph, monolayers do not present any shape change triggered by immersion in water. Conversely self-rolling is observed for the bilayer (Fig. 1B), and have been showed to form a tube directly in the first seconds after being immersed in water (Figure S2). When the bilayer is immersed in water, the difference of swelling degree between the H^+L and the H^-L leads the generation of the bending moment in the bilayer and its spontaneous rolling [23]. Previously reported study showed the H^+L and the H^-L layers are on the outer and the inner sides of the roll, respectively [14].

Based on the developed solvent-free film fabrication method, tuning layers' thickness lays on adjusting initial polymer content (Fig. 2D). Using aluminum mold of 43 mm diameter, it is possible to prepare thin films with thickness below 100 μm (respectively 89 ± 5 μm for the H^-L using 300 mg of polymer, and 82 ± 3 μm for the H^+L using 200 mg of polymer). Stable bilayer with tunable thickness can be prepared by adjusting the initial quantity of H^-L and H^+L polymer, using the same ratio. We showed that monolayers films conserve stable water content (Fig. 2C) even when varying initial polymer content. Indeed, the ANOVA studies revealed that there was no statistical difference in the equilibrium water content (%) when varying initial polymer content in each batch. This ensures the fabrication of thicker or thinner films, still conserving each layer properties and the water responsive self-rolling as presented in photographs of Fig. 2E. Below these masses, we noticed a bad distribution of the polymers following the solvent evaporation leading to non-homogeneous films when reticulated.

3.2. Loading and release studies

They are many ways of incorporating drug described in the literature: drugs loaded into films via *in situ* entrapment or post-fabrication equilibrium partitioning, drugs modified with a cross-linkable and cleavable linker that can be released once the tethers are degraded hydrolytically or enzymatically (tethering), or drugs pre-loaded into micro-particles that are subsequently entrapped in hydrogels (multiphase loading) [24].

We explored a simple entrapment method by immersion of cross-linked dry film in the drug solution for loading to ensure a rapid release of drug from the matrices. *In vitro* drug release experiments have been performed in PBS 1X. The reverse phase high performance liquid chromatography analytical method used for quantification provided the

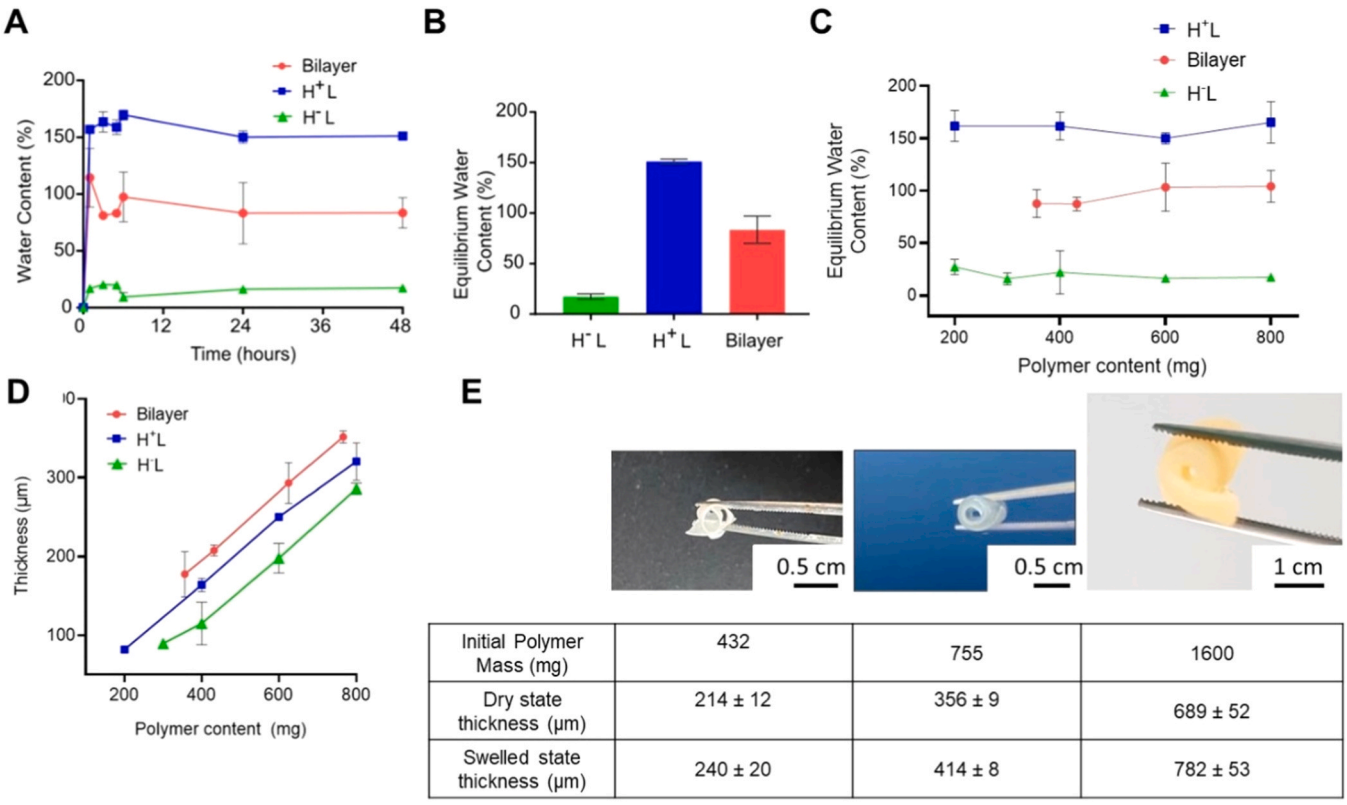

Initial Polymer Mass (mg)	432	755	1600
Dry state thickness (µm)	214 ± 12	356 ± 9	689 ± 52
Swelled state thickness (µm)	240 ± 20	414 ± 8	782 ± 53

Fig. 2. Characterization of UV crosslinked films. A- Water uptake kinetics of films after immersion in water. B- Equilibrium Water Content of films after 24 h in water showing the H⁻L behavior of $PEG_{8arm}10k\text{-}(PLA_{69})_8$ prepared film and the H⁺L one of $PEG_{8arm}10k\text{-}(PLA_{69})_8$ polymer film. **C**- Swelling ratio of monolayers with different initial polymer content: prepared films conserved stable swelling ratio when increasing polymer quantity. (One-way ANOVA and Tukey post-hoc test for multiple comparison for n=3) D- Thickness of film with different initial polymer content at dry state: increasing initial polymer quantity leads to the increase of reticulated film thickness. E- Thickness of bilayers in dry and swollen state showing tunable thickness by adjusting initial polymer quantity used, and regular thickness increase while varying the polymer content (layers size 1 cm x 1 cm). Data are expressed as mean ± SD (n = 3).

appropriate specificity, sensitivity, accuracy, and precision. Prednisolone due to its high carbon to heteroatom ratio can be separated through C18 column in reverse phase liquid chromatography. A full validation procedure was performed in accordance with International Conference on Harmonization of Technical Requirements for Registration of Pharmaceuticals for Human Use guidelines. The calibration curve was found to be linear over the concentration range of 0.1–100 µg/mL with regression coefficient of 0.9993. Limit of detection was found to be 0.03 µg/mL (signal to noise ratio of 3:1) and limit of quantification was found to be 0.10 µg/mL (signal to noise ratio of 10:1) (Table S3 and Figure S4).

Fig. 3 shows the time-dependent fractional release curves of prednisolone from simple monolayers H⁻L, H⁺L and from the bilayer. The amounts of drug released were normalized to the polymer dry mass of corresponding films to minimize the difference of mass between samples. The rate of release (M_t/M_∞) (%) was estimated as absolute cumulative amount of drug released at time *t* (M_t) proportionally to the total release amount at the end of the release process (M_∞).

Although they showed outwardly different water uptake behaviors, all three batches ensured comparable efficient prednisolone release for 264 hours, with an average 80 % release of encapsulated drug during the first 24 hours. For a more in-depth insight in the release, we considered t_{50} and t_{80} in this work, that correspond to the time at which respectively 50 % and 80 % of prednisolone was released, respectively. H⁻L, despite its reduced water uptake (17 ± 3 %) compared to the ones of the bilayer (5 times higher than 84 ± 16 %) and of the H⁺ L (9 times higher than 151 ± 3 %), showed to be efficient for drug release. The release of prednisolone was not significantly affected by the difference of equilibrium water content (%). Rapid matrices swelling during the first hour (Fig. 1A) lead to a burst release of 43 ± 8 % for the H⁻L, 64 ± 4 % for H⁺L and 38 ± 2 % for the bilayer. t_{50} was found to be lower than 1 hour for H⁺ L and between 1 and 2 hours for H⁻L and the bilayer. Nevertheless, since t_{80} and the trend of release curves were almost the same, it can be assumed that the release mechanism of prednisolone is the same for the three batches.

We also noticed at the end of the release process a higher prednisolone amount for the H⁺L copolymer which contains higher amount of PEG compared to the H⁻L (respectively 2.4 ±0.4 µg/mg vs 1.8 ± 0.1 µg/mg of polymer). This could be linked to the EG/LA molar ratio between the copolymers (EG/LA = 4.4 for H⁺L and 0.4 for H⁻L). The synthetized bilayer prepared using a ratio 1:1 of H⁻L and H⁺L presents a mean normalized release of 2.2 ± 0.2 µg of prednisolone per mg of polymer (Fig. 3C).

Different release models are referenced to describe the mechanism involved in released from polymers matrix [25]. Based on the shape of our experimental release kinetics curves the best fitting mathematical model was Korsmeyer Peppas model [26]. The values of *n* and *k* were obtained from the log-arithmetical curves of M_t/M_∞ as a function of time for each type of film and are given in Table 1.

It is important to mention that the Eq. (4) is restricted to the first 60 % of the released drug (linear part) [18]. Samples used in these experiments had square film shapes. The conceptual meanings of *n* is known to be dependent of the sample shape as reminded in Table S2 [27]. Release exponent on three batches was found to be inferior to 0.5, which indicates that drug release follows a Fickian mechanism. This means that the drug can quickly diffuse through the polymeric matrix because its hydrodynamic diameter is much smaller than the polymer network mesh size. The release is controlled, first, by

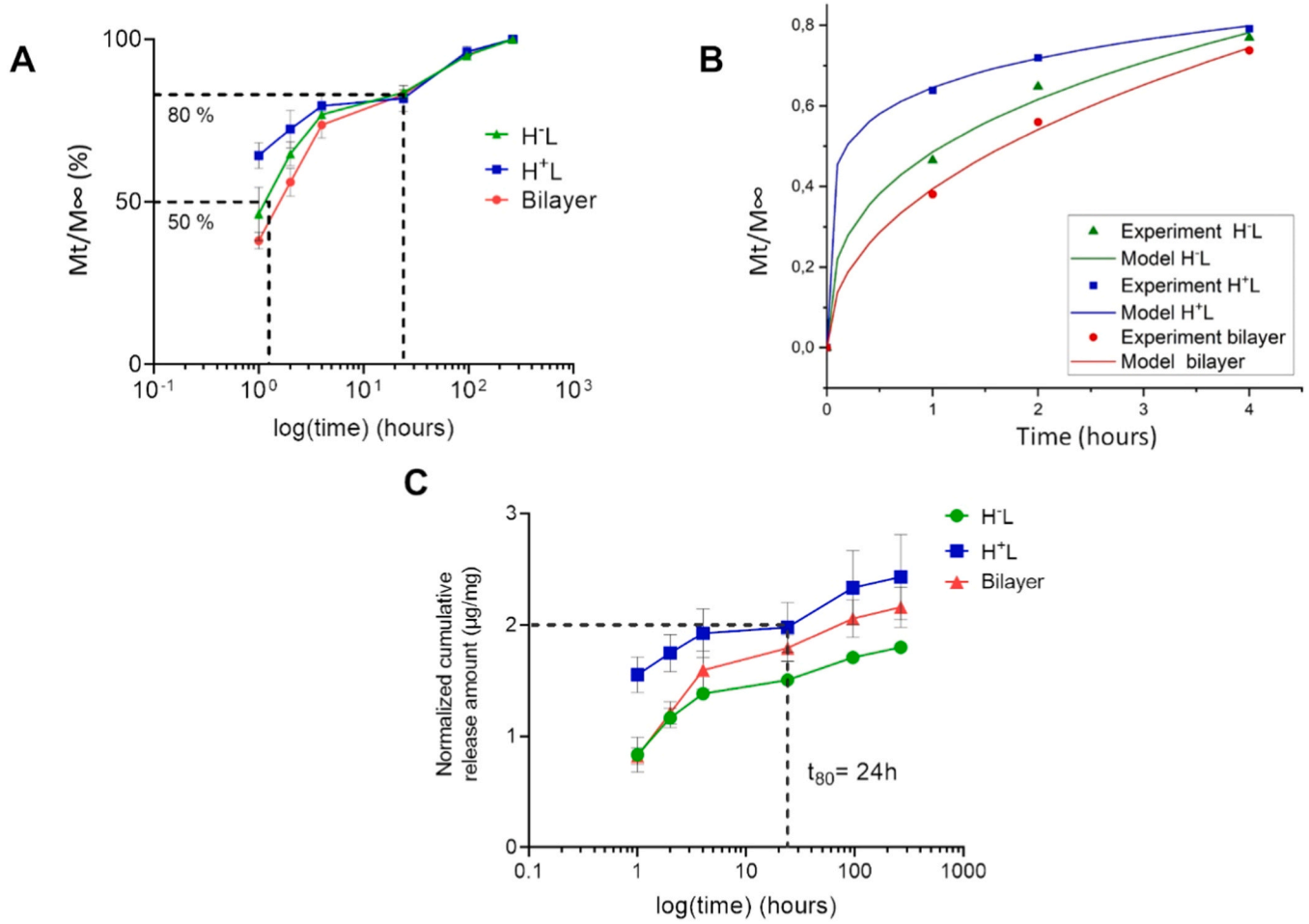

Fig. 3. A- Time-dependent release curves of prednisolone-loaded films presented as percentage of cumulative release M_t over total release M_∞. B- Fit of the Korsmeyer–Peppas model to experimentally determined prednisolone release kinetics from films on the first 60 % of release (curve= model, symbols= experimental points). C- Prednisolone normalized cumulative release vs log of time using water loading buffer containing 300 µg of drug in PBS 1X at 37°C (Thickness of samples; H^-L 136 ± 22 µm, H^+L 152 ± 12 µm, bilayer 241 ± 26 µm, values are expressed as mean ± SD, N=3).

Table 1
Kinetics parameters of prednisolone release from H^-L, H^+L and bilayer using Korsmeyer-Peppas model.

Parameters	H^-L	H^+L	Bilayer
R^2	0.9651	0.9928	0.9821
K	0.48 ± 0.04	0.64 ± 0.01	0.39 ± 0.05
n	0.35 ± 0.07	0.15 ± 0.01	0.46 ± 0.04

dissolution-diffusion of the drug in the swollen film, then by diffusion. The parameter *K* is correlated to the diffusion coefficient (D) of drug through the matrices. *K* is higher for H^+L (0.64 ± 0.01) which explains the faster prednisolone release during the first hour (Fig. 3A) observed for this film.

The main challenge in designing drug delivery systems is to deliver the drugs at the appropriate concentration. The aim of controlled release systems is to keep this suitable drug concentration in blood or in the colon for as long as possible. Oral prednisolone has a bioavailability of approximately 70 % and reaches a maximum plasmatic concentration (C_{max}) of 113–1343 ng/mL after a mean time (T_{max}) of 1–2.6 hours [28]. For example, Bashar et al. highlighted in their study a plasmatic concentration of 635 ± 125 ng/mL at a mean T_{max} of 2.21 hours for reference prednisolone provided after a single administration of 20 mg (study conducted on 14 participants with no evidence of clinically significant abnormal hematological, serum chemistry, and urine analysis values) [29]. Using water as loading buffer, we have reached with bilayers an average release of 216 ± 18 ng/mL per mg of polymer.

One way for increasing released amount, while conserving bilayers model is to improve the entrapped quantity in the matrices during loading process. For that, we investigated dissolving drug in a solvent with higher solubility than water. Indeed, prednisolone is slightly soluble in water (0.23 mg/mL in water) compared to other solvents: 33.33 mg/mL in ethanol, 20 mg/mL in acetone, and 5.55 mg/mL in chloroform [30].

The use of ethanol allows for the preparation of highly concentrated loading solutions. Release kinetics with ethanol showed to be similar to what was observed with water (Fig. 3B). In more details, 50 % of release was obtained after roughly 2 hours, and similarly 80 % of release was obtained after 24 hours. Korsmeyer-Peppas fitting analysis was also performed on this new set of release data and confirmed a Fickian diffusion whose parameters are summarized in Table 2. The values of *K* remained almost unchanged using initial prednisolone amount of 15 mg

Table 2
kinetics parameters of prednisolone release from bilayers with varying drug loading amount (Korsmeyer-Peppas model).

Parameters	15 mg	30 mg	60 mg
R^2	0.9864	0.9898	0.99957
K	0.31 ± 0.02	0.34 ± 0.02	0.42 ± 0.01
n	0.41 ± 0.04	0.44 ± 0.03	0.34 ± 0.01

and 30 mg which can be related to their similar rate of release (Fig. 4) compared to the batch loaded with 60 mg (0.42 ± 0.01). However, we observed that increasing drug loaded quantity did not influence the release mechanism; the release exponent on three batches was found to be inferior to 0.5. As expected, analysis showed an increase in total released amount when using more concentrated loading solutions. Referring to the known prednisolone pharmacokinetic parameters, we obtained in our studies normalized release of respectively 429 ± 65 ng/mL, 727 ± 10 ng/mL, and 1750 ± 122 ng/mL per mg of polymer by immersing films in ethanol solution containing 15 mg, 30 mg and 60 mg of drug in comparison with water.

In summary, our set of experimental data highlights the possibility of producing bilayers that allow for the delivery of prednisolone at levels sufficient to ensure a biological response. To further explore this aspect, the pharmacological effect of as-prepared bilayer was assessed by evaluating macrophages polarization in response to anti-inflammatory drug in pro-inflammatory condition [14,30].

3.3. Anti-inflammatory activity of released prednisolone

The anti-inflammatory activity of prednisolone released from the bilayers was assessed by analyzing cytokine IL1-β inhibition; one of the hallmarks of pro-inflammatory macrophages [31,32]. Macrophages are one of the most important cells of the immune system, present in most organs adapting to the local environment. They have both pro- or anti-inflammatory actions depending on their surrounding feedback [33]. Treatment with anti-inflammatory pharmaceuticals drugs, like prednisolone, are widely used for their therapeutic immune suppression. Thus, the anti-inflammatory activity of prednisolone released from bilayers in culture medium has been assessed by qPCR focusing on the inhibition of the IL-1β gene expression by RAW 264.7 macrophages upon an inflammatory stimulus triggered by the incubation with *E. coli* in vitro (Fig. 5). In untreated macrophages (control -), IL-1β transcripts if present, were under the threshold of detection. After bacteria exposure, IL-1 β transcripts were 8000 folds higher compared to untreated

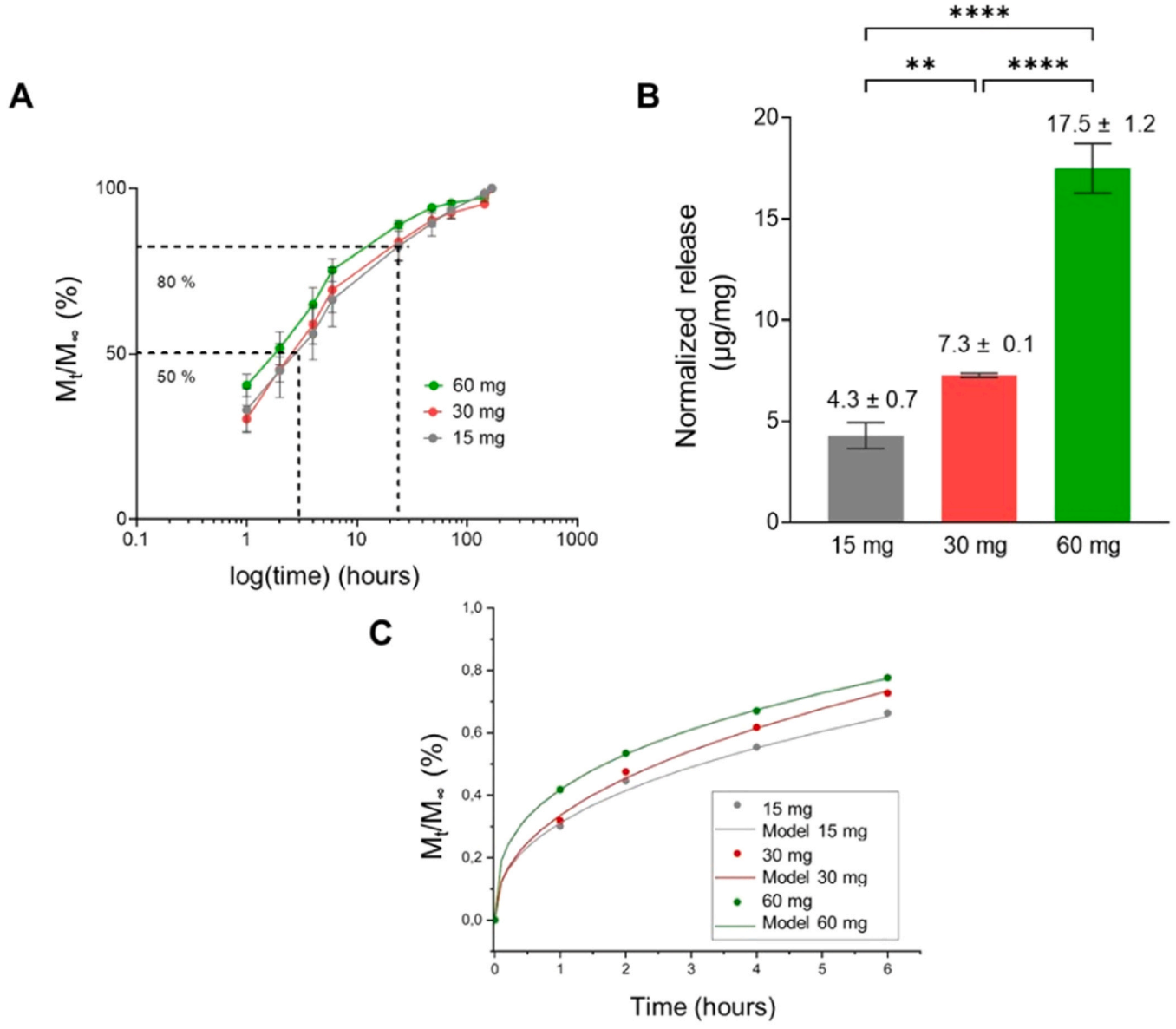

Fig. 4. A- Time-dependent release curves of prednisolone at 37°C presented as percentage of cumulative release M_t on total release M_∞ using increasing initial quantity in loading ethanol buffer 15 mg, 30 mg and 60 mg. B- Total normalized release of prednisolone from bilayers using ethanol loading solution containing 15 mg, 30 mg, and 60 mg (bilayers thickness 241 ± 26 µm, values are expressed as mean ± SD, n=3, one-way ANOVA with Tukey *post hoc* test, **p<0.01, ****p<0.0001). C- Fit of the Korsmeyer–Peppas model to experimentally determined prednisolone release kinetics from copolymers-based films on first 60 % of released solute (curve= model, symbols=experiment).

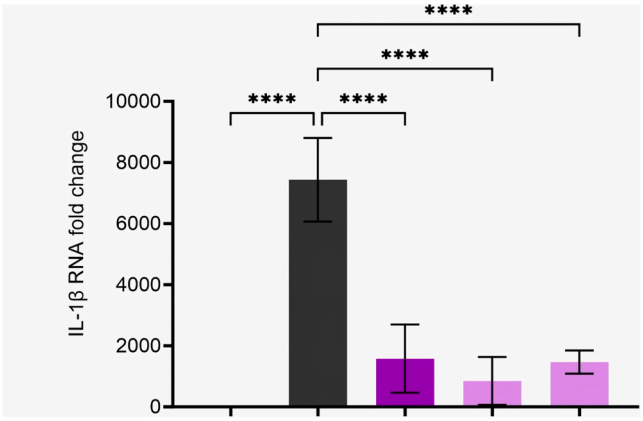

Bacteria	-	+	+	+	+
Prednisolone (μm)	0	0	30	12	25
Prednisolone source	N/A	N/A	in solution	in solution	in solution

Fold change (mean)	1	7435	1576	850	1466
Fold change (SD)	0	1368	1116	783	380

Fig. 5. Downregulation of IL-1β mRNA expression by bilayer released prednisolone. RAW 264.7 cells (5×10^5 cells/well) were stimulated by adding *E. coli BL21* strain and were further treated with free prednisolone (30 μM) or prednisolone released from bilayers (dry thickness = 253 ± 6 μm containing 12 μM and 25 μM of prednisolone equivalent) for 18 hours. Data are expressed as the mean ± SD of three independent experiments. Statistical analysis used a one-way ANOVA test followed by a *Tukey* post-hoc test (threshold of significance ****P<0.0001, ns: not significant, vs. control).

ones showing that macrophages with upregulation of pro-inflammatory cytokine IL-1β gene activation (control +). Then activated macrophages were cultured with prednisolone applied either in solution or released from our hydrogel bilayer. Whatever the source of prednisolone, IL-1β transcript levels in M1 macrophages were drastically downregulated, between 5 and 8 folds lower in average compared to activated M1 macrophages. No statistical differences were found neither relative to the different method of prednisolone exposure (in solution or released from bilayer) nor to the different concentrations examined (12, 25 and 30 μM). Altogether, this experiment demonstrates the anti-inflammatory activity of bilayer-released prednisolone. In conclusion, the results of the present study highlighted the possibility of preparing bilayers to target efficient drug release and modulate inflammatory gene expression. Our bilayers have proved their potential to deliver efficient anti-inflammatory drugs in vitro. Further experiments will be needed to confirm these preliminary but promising results for in vivo application.

4. Conclusion

We reported in this work a method to prepare bilayer constructs loaded with an anti-inflammatory drug and able to self-roll upon hydration. The bilayer construct was composed of an association of $PEG_{8arm}10k\text{-}(PLA_{69})_8$ hydrophobic layer and $PEG_{8arm}20k\text{-}(PLA_{13})_8$ hydrophilic layer allowing the fabrication of a non-cytotoxic prednisolone-loaded and less-invasive device with tunable shape and scales, via a simple and fast processing route. The construct bilayer spontaneously rolled up to form in tube directly after immersion in water due to the difference of water uptake between the hydrophilic and hydrophobic layers entering in its composition.

The *in vitro* release studies fitted with Korsmeyer-Peppas model confirmed a drug release mechanism via Fickian diffusion ($n < 0.5$). The total released amount could be optimized by choosing ethanol as the solvent of loading to ensure higher entrapment in the bilayer construct up to 17.5 ± 1.2 μg of prednisolone per mg of polymer. We also showed the efficient anti-inflammatory properties of the released prednisolone by down-regulating pro-inflammatory IL-1β gene expression in murine macrophages upon a strong pro-inflammatory stimulus. Taken together, these results indicate that the designed bilayers are biologically relevant and could have great pharmacological potential as medical devices able to deliver therapeutic doses of drugs in local biological environments.

CRediT authorship contribution statement

Katia Carneiro: Writing – review & editing, Investigation, Conceptualization. **Valeriy Luchnikov:** Writing – review & editing, Conceptualization. **Noëlle Mathieu:** Writing – review & editing, Project administration, Funding acquisition, Conceptualization. **Xavier Garric:** Visualization. **Benjamin Nottelet:** Writing – review & editing, Project administration, Funding acquisition, Conceptualization. **Karine Anselme:** Writing – review & editing, Project administration, Funding acquisition, Conceptualization. **Laurent Pieuchot:** Writing – review & editing, Conceptualization. **Arnaud Ponche:** Writing – review & editing, Supervision, Conceptualization. **Sidzigui Ouedraogo:** Writing – original draft, Investigation. **Mathilde Grosjean:** Investigation. **Isabelle Brigaud:** Writing – review & editing, Investigation.

Declaration of Competing Interest

The authors declare that they have no known competing financial interests or personal relationships that could have appeared to influence the work reported in this paper.

Data availability

Data will be made available on request.

Acknowledgement

This work was supported by the ANR2019-OPENN held by the University of Montpellier (ANR-19-CE19–0022–02), CNRS (ANR-19-CE19–0022–03), IRSN (ANR-19-CE19–0022–01), and Institut Carnot MICA (COROL-2019).

Appendix A. Supporting information

Supplementary data associated with this article can be found in the online version at doi:10.1016/j.colsurfb.2024.114039.

References

[1] L. Moussa, G. Pattappa, B. Doix, S.-L. Benselama, C. Demarquay, M. Benderitter, A. Sémont, R. Tamarat, J. Guicheux, P. Weiss, G. Réthoré, N. Mathieu, A biomaterial-assisted mesenchymal stromal cell therapy alleviates colonic radiation-induced damage, Biomaterials 115 (2017) 40–52, https://doi.org/10.1016/j.biomaterials.2016.11.017.
[2] H.J.N. Andreyev, P. Vlavianos, P. Blake, D. Dearnaley, A.R. Norman, D. Tait, Gastrointestinal symptoms after pelvic radiotherapy: role for the gastroenterologist? Int. J. Radiat. Oncol. Biol. Phys. 62 (2005) 1464–1471, https://doi.org/10.1016/j.ijrobp.2004.12.087.
[3] H.J.N. Andreyev, A. Wotherspoon, J.W. Denham, M. Hauer-Jensen, Pelvic radiation disease: new understanding and new solutions for a new disease in the era of cancer survivorship, Scand. J. Gastroenterol. 46 (2011) 389–397, https://doi.org/10.3109/00365521.2010.545832.
[4] H.J.N. Andreyev, A. Wotherspoon, J.W. Denham, M. Hauer-Jensen, Defining pelvic-radiation disease for the survivorship era, Lancet Oncol. 11 (2010) 310–312, https://doi.org/10.1016/S1470-2045(10)70026-7.
[5] L. Fuccio, A. Guido, H.J.N. Andreyev, Management of intestinal complications in patients with pelvic radiation disease, Clin. Gastroenterol. Hepatol. 10 (2012) 1326–1334.e4, https://doi.org/10.1016/J.CGH.2012.07.017.
[6] L. Moussa, B. Usunier, C. Demarquay, M. Benderitter, R. Tamarat, A. Sémont, N. Mathieu, Bowel radiation injury: complexity of the pathophysiology and promises of cell and tissue engineering, Cell Transpl. 25 (2016) 1723–1746, https://doi.org/10.3727/096368916×691664.

[7] S. Moghadam-kia, V.P. Werth, Prevention and treatment of systemic glucocorticoid side effects, (2010) 239–248.
[8] L. Liu, A. Ghaemi, S. Gekle, S. Agarwal, One-component dual actuation: poly (NIPAM) can actuate to stable 3D forms with reversible size change, Adv. Mater. 28 (2016) 9792–9796, https://doi.org/10.1002/adma.201603677.
[9] E. Wisotzki, A. Thissen, A.B.M.O. Islam, A. Klein, W. Jaegermann, R. Rudolph, D. Tonti, C. Pettenkofer, S. Sci, B. Valeriy Luchnikov, O. Sydorenko, M. Stamm, Self-Rolled Polymer and Composite Polymer/Metal Micro-and Nanotubes with Patterned Inner Walls**, 515 (2002). https://doi.org/10.1002/adma.200401836.
[10] V. Luchnikov, L. Lonov, M. Stamm, Self-rolled polymer tubes: Novel tools for microfluidics, microbiology, and drug-delivery systems, Macromol. Rapid Commun. 32 (2011) 1943–1952, https://doi.org/10.1002/marc.201100482.
[11] S.Y. Zheng, Y. Tian, X.N. Zhang, M. Du, Y. Song, Z.L. Wu, Q. Zheng, Spin-coating-assisted fabrication of ultrathin physical hydrogel films with high toughness and fast response, Soft Matter 14 (2018) 5888–5897, https://doi.org/10.1039/c8sm01126e.
[12] R.Z. Xiao, Z.W. Zeng, G.L. Zhou, J.J. Wang, F.Z. Li, A.M. Wang, Recent advances in PEG-PLA block copolymer nanoparticles, Int. J. Nanomed. 5 (2010) 1057–1065, https://doi.org/10.2147/IJN.S14912.
[13] A. Harrane, A. Leroy, H. Nouailhas, X. Garric, J. Coudane, B. Nottelet, PLA-based biodegradable and tunable soft elastomers for biomedical applications, Biomed. Mater. 6 (2011), https://doi.org/10.1088/1748-6041/6/6/065006.
[14] M. Grosjean, S. Ouedraogo, S. Déjean, X. Garric, V. Luchnikov, A. Ponche, N. Mathieu, K. Anselme, B. Nottelet, Bioresorbable bilayered elastomer/hydrogel constructs with gradual interfaces for the fast actuation of self-rolling tubes, ACS Appl. Mater. Interfaces 14 (2022) 43719–43731, https://doi.org/10.1021/acsami.2c11264.
[15] B. Kim, Y. Son, M. Kim, K. Kim, Prednisolone suppresses the immunostimulatory effects of 27-hydroxycholesterol, Exp. Ther. Med. (2020) 2335–2342, https://doi.org/10.3892/etm.2020.8458.
[16] A.K. Andersson, M.V. Chaduvula, S.E. Atkinson, S. Khanolkar-Young, S. Jain, L. Suneetha, S. Suneetha, D.N.J. Lockwood, Effects of prednisolone treatment on cytokine expression in patients with leprosy type 1 reactions, Infect. Immun. 73 (2005) 3725, https://doi.org/10.1128/IAI.73.6.3725-3733.2005.
[17] T. Huang, K. Anselme, S. Sarrailh, A. Ponche, High-performance liquid chromatography as a technique to determine protein adsorption onto hydrophilic/hydrophobic surfaces, Int. J. Pharm. 497 (2016) 54–61, https://doi.org/10.1016/j.ijpharm.2015.11.013.
[18] E.T. Tenório-Neto, D.D.S. Lima, M.R. Guilherme, M.K. Lima-Tenório, D.B. Scariot, C.V. Nakamura, M.H. Kunita, A.F. Rubira, Synthesis and drug release profile of a dual-responsive poly(ethylene glycol) hydrogel nanocomposite, RSC Adv. 7 (2017) 27637–27644, https://doi.org/10.1039/c7ra02846f.
[19] S. Kiriakidis, E. Andreakos, C. Monaco, B. Foxwell, M. Feldmann, E. Paleolog, VEGF expression in human macrophages is NF-κB-dependent: studies using adenoviruses expressing the endogenous NF-κB inhibitor IκBα and a kinase-defective form of the IκB kinase 2, J. Cell Sci. 116 (2003) 665–674, https://doi.org/10.1242/JCS.00286.
[20] K.J. Livak, T.D. Schmittgen, Analysis of relative gene expression data using real-time quantitative PCR and the 2-ΔΔCT method, Methods 25 (2001) 402–408, https://doi.org/10.1006/meth.2001.1262.
[21] B.W. Hwang, Y.E. Kim, M. Kim, S. Han, S. Bok, K.M. Park, A. Shrinidhi, K.S. Kim, G. O. Ahn, S.K. Hahn, Supramolecular hydrogels encapsulating bioengineered mesenchymal stem cells for ischemic therapy, RSC Adv. 8 (2018) 18771–18775, https://doi.org/10.1039/c8ra00464a.
[22] R. Joshi, W. Akram, R. Chauhan, N. Garud, R. Joshi, W. Akram, R. Chauhan, N. Garud, Thin Films: A Promising Approach for Drug Delivery System, Drug Carriers [Working Title] (2022). https://doi.org/10.5772/INTECHOPEN.103793.
[23] L. Ionov, Hydrogel-based actuators: possibilities and limitations, Mater. Today 17 (2014) 494–503, https://doi.org/10.1016/j.mattod.2014.07.002.
[24] C.C. Lin, K.S. Anseth, PEG hydrogels for the controlled release of biomolecules in regenerative medicine, Pharm. Res. 26 (2009) 631–643, https://doi.org/10.1007/s11095-008-9801-2.
[25] M. Vigata, C. Meinert, D.W. Hutmacher, N. Bock, Hydrogels as drug delivery systems: a review of current characterization and evaluation techniques, Pharmaceutics 12 (2020) 1–45, https://doi.org/10.3390/pharmaceutics12121188.
[26] S. Nawaz, S. Khan, U. Farooq, M.S. Haider, N.M. Ranjha, A. Rasul, A. Nawaz, N. Arshad, R. Hameed, Biocompatible hydrogels for the controlled delivery of anti-hypertensive agent: development, characterization and in vitro evaluation, Des. Monomers Polym. 21 (2018) 18–32, https://doi.org/10.1080/15685551.2018.1445416.
[27] J. Siepmann, F. Siepmann, Mathematical modeling of drug delivery, Int. J. Pharm. 364 (2008) 328–343, https://doi.org/10.1016/j.ijpharm.2008.09.004.
[28] J.J. Ferry, E.C. Heath, C.F. Ryan, Relative and Absolute Bioavailability of Prednisone and Prednisolone After Separate Oral and Intravenous Doses, (1988) 81–87.
[29] T. Bashar, M.N.H. Apu, M.S. Mostaid, M.S. Islam, A. Hasnat, Pharmacokinetics and bioavailability study of a prednisolone tablet as a single oral dose in bangladeshi healthy volunteers, Dose Response 16 (2018), https://doi.org/10.1177/1559325818783932.
[30] S.L. Ali, Z.D. Apotheker, Syed Laik Ali Zentrallaboratorium Deutscher Apotheker 6236 Eschborn Germany, 21 (1992).
[31] M. Cabanel, T. Pinheiro, M. Cury, E.L. Cheikh, K. Carneiro, The epigenome as a putative target for skin repair: the HDAC inhibitor Trichostatin A modulates myeloid progenitor plasticity and behavior and improves wound healing, J. Transl. Med. (2019) 1–13, https://doi.org/10.1186/s12967-019-1998-9.
[32] Y. Liu, X. Zou, Y. Chai, Y. Yao, Macrophage polarization in inflammatory diseases 10 (2014), https://doi.org/10.7150/ijbs.8879.
[33] C. Yunna, H. Mengru, W. Lei, C. Weidong, Macrophage M1/M2 polarization, Eur. J. Pharmacol. 877 (2020) 173090, https://doi.org/10.1016/j.ejphar.2020.173090.